The effect of prolonged drought and recovery on soil VOC fluxes in an experimental rainforest

Giovanni Pugliese (G.Pugliese@mpic.de)
Max Planck Institute for Chemistry https://orcid.org/0000-0002-2869-3588
Johannes Ingrisch
University of Innsbruck
Laura K. Meredith
University of Arizona
Eva Y. Pfannerstill
Max Planck Institute for Chemistry https://orcid.org/0000-0001-7715-1200
Thomas Klüpfel
Max Planck Institute for Chemistry
Kathiravan Meeran
University of Innsbruck https://orcid.org/0000-0002-3987-5002
Joseph Byron
Max Planck Institute for Chemistry
Gemma Purser
UK Centre for Ecology & Hydrology
Juliana Gil-Loaiza
University of Arizona
Joost van Haren
University of Arizona
Juergen Kreuzwieser
University of Freiburg https://orcid.org/0000-0002-5251-9723
S. Nemiah Ladd
University of Basel https://orcid.org/0000-0002-0132-5785
Christiane Werner
University of Freiburg https://orcid.org/0000-0002-7676-9057
Jonathan Williams
Max Planck Institut für Chemie https://orcid.org/0000-0001-9421-1703

Article

Keywords:

Posted Date: September 15th, 2022

DOI: https://doi.org/10.21203/rs.3.rs-2025580/v1

The effect of prolonged drought and recovery on soil VOC fluxes in an experimental rainforest

Giovanni Pugliese[1,2], Johannes Ingrisch[3], Laura K. Meredith[4,5], Eva Y. Pfannerstill[2]*, Thomas Klüpfel[2], Kathiravan Meeran[3], Joseph Byron[2], Gemma Purser[6, 7], Juliana Gil-Loaiza[4], Joost van Haren[4,5,8], Jürgen Kreuzwieser[1], S. Nemiah Ladd[1,9], Christiane Werner[1], and Jonathan Williams[2]

[1]Ecosystem Physiology, Faculty of Environment and Natural Resources, University of Freiburg, Freiburg, Germany

[2]Atmospheric Chemistry Department, Max Planck Institute for Chemistry, Mainz, Germany

[3]Institute of Ecology, University of Innsbruck, Innsbruck, Austria

[4]School of Natural Resources and the Environment, University of Arizona, Tucson, Arizona, USA

[5]Biosphere 2, University of Arizona, Oracle, AZ, USA

[6]UK Centre for Ecology & Hydrology, Penicuik, Edinburgh, UK

[7]School of Chemistry, The University of Edinburgh, Edinburgh, UK

[8]Honors College, University of Arizona, Tucson, Arizona, USA

[9]Department of Environmental Sciences, University of Basel, Basel, Switzerland

*now at: Department of Environmental Science, Policy, and Management, University of California at Berkeley, Berkeley, CA, USA

*Corresponding author: g.pugliese@mpic.de (ORCID: https://orcid.org/0000-0002-2869-3588)

1. Abstract

Drought can affect the capacity of soils to emit and consume biogenic volatile organic compounds (VOCs). Here we show the impact of prolonged drought followed by rain and recovery on soil VOC fluxes from an experimental rainforest. Under wet conditions the rainforest soil acted as a net VOCs sink, in particular for isoprenoids, carbonyls and alcohols. The sink capacity decreased progressively during drought, and at soil moistures below ~19% the soil became a source of several VOCs. Position specific ^{13}C-pyruvate labelling experiments revealed that soil microbes were responsible for the emissions and that energetic investment in VOC production increased during drought. Soil rewetting induced an emission pulse of carbonyls and dimethyl sulfide due to water-induced mobilization of carbon and sulfur pools of soil organic matter. Results show that, the extended drought periods predicted for tropical rainforest regions will strongly affect soil VOC fluxes thereby impacting atmospheric chemistry and climate.

2. Introduction

Atmospheric biogenic volatile organic compounds (VOCs) are emitted and taken up by terrestrial ecosystems and play an important role in determining atmospheric processes that control air quality and climate. They react readily with the primary atmospheric oxidants hydroxyl radicals (OH) and ozone (O_3) leading to the production of secondary organic aerosol (SOA) particles. Such particles can in turn affect cloud formation, the earth's radiative balance and thereby climate[1]. Current global atmospheric models consider plants as the only source and sink of atmospheric VOCs, neglecting any influence from soils[2,3]. However, recent studies have shown that under certain condition the soils contribution to total ecosystem VOC budget can even be comparable to that of the plants[4–7]. They therefore represent an important component of the overall ecosystem VOC dynamic.

Soil VOC fluxes are inherently uncertain since they are the combined result of numerous biotic and abiotic processes. Biotic processes include microbial uptake, microbial decomposition of soil organic carbon (SOC) and plant residues, as well as emission from plant roots; while the abiotic processes include dissolution in or evaporation from soil water, adsorption to soil particles, reaction with soil chemicals, and evaporation from leaf litter[8–10]. Soil biotic and abiotic processes are in turn dependent on soil physio-chemical properties and environmental factors, e.g., temperature, soil pH, soil moisture, soil texture, soil porosity, nutrients, and SOC content. As a result, large variations in the composition, magnitude, and direction (i.e. emission vs uptake) of soil VOC fluxes have been observed as a function of ecosystem, season, diel dynamics, and environmental conditions[11–15].

The strong dependency of soil VOC fluxes on environmental conditions highlights the need to understand how soil VOC fluxes will change in response to human-accelerated climate change. Among the predicted impacts of climate change, is that drought frequency and duration will increase worldwide[16]. Such events can potentially affect soil VOC fluxes, impacting the atmospheric budgets of certain VOCs with further and unpredictable consequences on climate. This is particularly relevant for tropical rainforests, which represent the largest source (about 70%) of biogenic VOCs[2,3].

In this study, we conducted a unique long-term drought experiment (B2-WALD campaign[17]) in the enclosed experimental rainforest of the biosphere 2 (B2 TRF, Arizona, USA), to assess the effects of prolonged and severe drought on soil VOC fluxes direction and magnitude. The ability to control and manipulate ecosystem conditions makes the B2 TRF an ideal site to study VOC dynamics[18–20]. Moreover, UV light filtering by the glass of the biosphere and the low ozone concentration in the ambient air, precluded any complication of emission signals through atmospheric oxidation chemistry. To characterize the origin of emitted VOCs, we conducted additional tracer experiments with position-specific ^{13}C-labelled pyruvate both during pre-drought and during drought. During the entire

campaign, soil respiration, soil temperature, soil moisture and soil matric potential were also measured and their effects on long term and diel soil VOC flux dynamics were analyzed.

3. Results

3.1 Long term soil VOC fluxes dynamics

Soil moisture and soil matric potential decreased strongly as the drought progressed, from 29 to 12.5% and from 0 to -3.7 MPa, respectively, but recovered back to pre-drought levels after the rewetting rain events. In contrast, soil temperature was relatively stable throughout the campaign (21.5- 25.5°C) with little diel dynamics (1.4 ± 4°C). Soil respiration (Figure 1) decreased similarly to the soil moisture, indicating that the soil microbial activity and root respiration decreased due to a reduction in soil water content[17,21].

Soil VOC fluxes showed distinct variations associated with the different periods of the campaign (Figure 2). Generally, the B2 TRF soil acted as a strong net sink for all measured isoprenoid compounds namely isoprene, monoterpenes, and the isoprene oxidation products C_5H_8O and methacrolein plus methyl vinyl ketone (MACR+MVK; both measured at *m/z* 71.049), with isoprene (C_5H_8) showing the highest net sink (Figure 2, blue plots). Two types of temporal patterns were detected in the isoprenoids, namely the one displayed by isoprene and C_5H_8O and the other by monoterpenes and MACR+MVK. Soil uptake of isoprene and C_5H_8O peaked one week after the onset of the drought, then it steady decreased with the development of the drought, but increased back to pre-drought levels during the rewetting period. Soil uptake of isoprene and C_5H_8O can be attributed to the soil microbiome[10,19,22]. The fact that the soil uptake of these two VOCs decreased similarly to respiration in response to drought, can be seen as further evidence that the soil consumption of both VOCs was linked to the soil microbial activity. In contrast to isoprene and C_5H_8O, soil uptake of monoterpenes and MACR+MVK slightly increased during the drought. A possible explanation is that the microbes consuming isoprene/C_5H_8O were more affected by drought than those consuming monoterpenes/MACR+MVK. Another possible explanation would be that the increased ambient air concentrations of monoterpenes and MACR+MVK (Figure S1) during the drought may have induced an adaptation of the soil microbiome to consume these compounds at a relatively higher rate. Periodically, isolated soil flux measurements of speciated monoterpenes were made from manual soil chambers by GC-MS. These indicated that the uptake of the sum of monoterpenes measured by PTR-ToF-MS was mainly driven by (-)-α-pinene and (-)-β-pinene (Figure S2). These two monoterpene enantiomers were the strongest emitted by the vegetation in the B2 TRF[23]. In addition, GC-MS measurements showed that although the total monoterpenes fluxes resulted in a net uptake throughout the campaign, some monoterpenes such as terpinolene, γ-terpinolene, α-terpinene were mostly emitted by the soil. Soil emissions of monoterpenes have previously been observed in several

ecosystems and have been attributed to microbial litter decomposition and to plant root emissions[24,25]. Considering the total monoterpenes flux, GC-MS and PTR-ToF-MS measurements showed a very similar trend and magnitude confirming the reliability of both measurement methods. Soil fluxes of the carbonyl compounds acetone, acetaldehyde, butanone and pentanone all showed similar temporal variation patterns (Figure 2, green plots), which differed from the aforementioned isoprenoid patterns. All carbonyls were taken up by the soil during the pre-drought period but as the drought progressed, the uptake gradually switched to emissions. Hence, the soil became a source of carbonyl compounds under severe drought. Apart from butanone, all carbonyls showed a large emission peak immediately after the first rain event. Shortly after rewetting, all carbonyls shifted to be taken up by the soil again at rates about 10 times higher than pre-drought, but then the uptake steadily decreased to pre-drought levels. As observed for the isoprenoids, soil uptake capacity of all carbonyls during pre-drought and during recovery period can be attributable to the higher microbial activity in wet soil compared to dry soil, although it cannot be excluded that their abiotic dissolution in the wet soil may have contributed to the total uptake. The gradual increase in soil emissions of all carbonyl compounds with increasing drought could be due to their production by soil microbes from soil organic matter as protective molecules in response to drought stress. Microbes under drought stress are known to generate high concentrations of chemicals internally in order to increase the osmotic potential of the cell and thereby draw more water from the surroundings[26].

Another distinct temporal pattern was identified for the two alcohols methanol and ethanol (Figure 2, dark green plots) which were mostly taken up by the soil throughout the campaign. Their uptake slightly increased as the drought progressed but strongly increased after the two rain events. Soil uptake of methanol and ethanol during the whole campaign is also attributable to the soil microbial activity. A wide range of soil microorganisms utilize ethanol and methanol as a carbon and energy source under both oxic and anoxic conditions[27,28] causing a net uptake in soil in diverse ecosystems and conditions[6,11,29,30]. The higher soil uptake capacity observed for both alcohols during the recovery period, could be due to the synergistic effect of an increased microbial activity, an increase abiotic dissolution in wet soil and increased ambient air concentrations (Figure S1).

Soil fluxes were also detected for the sulfur containing compound dimethyl sulfide (Figure 2, red plot). Dimethyl sulfide was taken up (~0.01 μmol m^{-2} h^{-1}) by the soil during the pre-drought and mild-drought periods, but was weakly emitted (~0.005 μmol m^{-2} h^{-1}) during the severe drought period. It showed two emission peaks directly after the rain events: up to 0.18 μmol m^{-2} h^{-1} after the first rain event and up to 0.05 μmol m^{-2} h^{-1} after the second rain event. Dimethyl sulfide production in soil has been attributed to the microbial metabolism of sulfur-containing compounds from the soil organic matter [31–34].The associated increase also observed in ambient concentrations (Figure S1) after both the first

and the second rain events clearly showed that soil can significantly contribute to dimethyl sulfide concentrations in the atmosphere.

The nitrogen containing compound methyl nitrite, CH_3ONO (Figure 2, yellow plot) was also exchanged by the soil. This compound showed weak and highly variable fluxes both in and out of the soil during the pre-drought and mild drought periods. However, with the onset of severe drought methyl nitrite was consistently emitted, and flux rates increased up to 0.025 μmol m^{-2} h^{-1}. During the recovery period methyl nitrite emission decreased steadily back to pre-drought levels. The observed methyl nitrite emission during severe drought is new and of potential significance to atmospheric chemistry in forests under drought stress as this molecule is readily photolyzed (lifetime ca. 2 minutes) to generate NO and formaldehyde[35]. The observed emission could be due to the reaction between nitrous acid (HONO) and lignin, which is one of the major constituents of the soil organic matter[36,37]. Increased HONO emissions when the soils dry out have been widely reported and associated to soil pH, chemical equilibrium with soil nitrite, heterogeneous hydrolysis of hydroxylamine, and to the release by soil ammonia-oxidizing microbes[38–41].

It should be noted that soil VOC uptake rates are both function of soil process and ambient concentration above the soil (Figure S1). To focus on soil process changes induced by the drought stages and avoid confounding effects by changes in VOC ambient concentrations, for those compounds that were taken up by the soil, we calculated deposition velocities (Figure S3), which are defined as the ratio of VOC uptake rates and their ambient concentrations. Although the deposition velocities trends were very similar to those of the net fluxes, it is evident that some variations observed in net soil uptakes were driven by changes in VOCs concentration in the atmosphere above the soil rather than by an increase in soil uptake capacity. For instance, isoprene soil deposition velocity shows that after the rain event the isoprene soil uptake capacity recovered to pre-drought levels and that the lower net isoprene uptake observed during the recovery period compared to the pre-drought period was due to a lower isoprene concentration in the ambient air.

Soil moisture was a key driver for VOC fluxes and the relationship between VOC fluxes/deposition velocities and soil moisture was non-linear evolving around a soil moisture threshold of ~19%, as determined by segmented regression (Figure 3a-b). Below this soil moisture threshold, isoprene uptake substantially declined and butanone, methyl nitrite and C_5H_8O shifted from uptake to emission. This suggests that 19% represents the soil moisture threshold corresponding to the point when the water-stressed soil microbes started producing and accumulating protective osmolytes, including VOCs, to reduce their internal water potential to avoid dehydrating and dying[26,42].

3.2 Rewet dynamics

Temporal dynamics of soil respiration and soil VOC fluxes following soil rewetting events were analyzed in detail (Figure 4). To capture fast soil flux rewet dynamics, 3 soil chambers placed on 3 different sites of the B2 TRF were manually rewetted at 5:30 am on 12 December 2019 and for the following 5 hours were measured with a high frequency, i.e. each chamber was measured every 30 minutes (Figure 4a). At 11 am on 12 December 2019, the remaining 9 chambers were subjected to the first whole forest rain rewet (Figure 4b) involving simulated rainfall from the roof mounted sprinkler system, while the 3 manually rewetted chambers were covered with rainout shelters. From 30 minutes before the whole forest rewet, all the 12 chambers where measured consecutively with a temporal resolution of 2 hours. A second rainfall event on the whole forest involving all 12 soil chambers was conducted one week later on 19 December 2019 at 11:00 (Figure 4c).

A pulse in CO_2 soil emissions was observed after all rewet events (Figure 4, black plots). This phenomenon is known as the "Birch effect" and has been attributed to a rewetting-induced mineralization of labile soil organic carbon pools[43–45]. The increased availability of these organic substrates after the rewet is thought to be due to an increased release of intracellular osmolytes accumulated by water-stressed microorganisms, to microbial cell lysis caused by osmotic shock, and to the physical disruption of soil aggregates protecting organic matter[26,46,47]. An emission pulse was also observed for dimethyl sulfide (Figure 4, red plots) after all rewet events, and for carbonyl compounds (Figure 4, light green plots) after the rewet events on 12 December. The carbonyls pulse was observed within 4 hours after the manual rewet and within 2 hours after the first rain rewet and, in general, it occurred about 12 hours earlier than the CO_2 pulse. This suggest that carbonyls pulse was generated by the immediate water-induced mobilization of the soil organic carbon while the CO_2 pulse, as previously stated, was the result of the subsequent microbial mineralization of the mobilized organic substrates. The dimethyl sulfide pulse is attributable to a water induced mobilization of the soil organic sulfur pools, whereby large insoluble sulfur-containing organic molecules are reduced to smaller soluble sulfur containing molecules by soil microbes or by extra cellular soil enzyme[48,49]. As the dimethyl sulfide pulse occurred about 7 hours later than carbonyls pulse, it suggests that the sulfur pools mobilization occurred in general later than the carbon pools mobilization or that dimethyl sulfide, compared to carbonyls, was generated from the degradation of more recalcitrant substances. As shown in Figure 1 for CO_2 and in Figure 2 for dimethyl sulfide, the emission pulses following the second rain event were significantly lower in absolute magnitude compared to the pulses following the first rain rewet, indicating that shorter drought-rewet cycles induce a lower mobilization and mineralization of the soil organic matter or that induce a lower build-up of substrate pools[50–52]. Indeed,

197 the subsequent rain events conducted every second day starting from 21 December did not induce
198 any VOCs and CO_2 soil emission pulses.
199 The soil uptake rates of isoprene, C_5H_8O and monoterpenes increased considerably only the day after
200 the rewets (Figure 4, blue plots), reflecting the time needed for the microbes responsible for the
201 consumption of these compounds to restart their activity. In contrast, the uptake of MACR+MVK
202 peaked within a few hours after the rewet events most probably due to its abiotic dissolution in wet
203 soil. An increase in soil uptake of alcohols was observed within 4 hours after the rewets (Figure 4, dark
204 green plots) as a consequence of the simultaneous increase in their ambient concentrations (Figure
205 S1) and to their abiotic dissolution in wet soil. Methyl nitrite emission (Figure 4, dark yellow plots)
206 slowly decreased in response to the rewets likely as a consequence of decreasing HONO production
207 with increasing soil moisture[39].

208 ## 3.3 Diel dynamics

209 Diel dynamics of soil VOC fluxes, deposition velocities and environmental variables were analyzed for
210 each period of the campaign (Figure 5). As exemplified for isoprene (Figure 5a), soil fluxes of all
211 isoprenoids showed a daytime maximum and minimum uptake rates at night, closely following the
212 diel cycle of their ambient concentrations (Figure 5b). A similar diel cycle was observed during the
213 recovery period for acetone, acetaldehyde, butanone, pentanone and methanol, all of which were
214 taken up by the soil (Figure S4). In contrast, the soil emissions of carbonyl compounds as well as those
215 of dimethyl sulfide did not show any diel cycle. A diel cycle was also observed for isoprenoid deposition
216 velocities (Figure 5c) and methyl nitrite emissions (Figure 5d).
217 In order to identify potential process drivers, a correlation analysis of the average hourly values was
218 performed between environmental factors that followed a diel cycle (i.e. soil temperature (Figure 5f)
219 and soil matric potential (Figure 5g)) and soil VOCs fluxes and deposition velocities. A clockwise
220 hysteresis was observed for the relationship between isoprene deposition and soil matric potential
221 and between methyl nitrite emission and soil matric potential (Figure 6a), as well as for the
222 relationship between isoprene deposition and soil temperature, and between methyl nitrite emission
223 and soil temperature (Figure 6b), indicating that the observed diel cycles of VOC fluxes were not driven
224 by these environmental factors. The decrease observed in isoprenoid deposition velocity during the
225 night was most probably due to substrate limitation in a very depleted ambient air at night as shown
226 in Figure 5b. Higher daytime emission of methyl nitrite compared to nighttime can be attributed to a
227 higher HONO production during the day which has been attributed to a photo-enhanced conversion
228 of NO_2 or nitrate photolysis on the soil[53,54].

3.4 Origin of VOC emissions

To identify the origin of the emitted VOCs, the soil was labeled with position specific $^{13}C_1$-pyruvate and $^{13}C_2$-pyruvate. A net soil emission was observed for ^{13}C-enriched acetone after $^{13}C_2$-pyruvate injections both during pre-drought and during drought period (Figure 7). This is strong evidence that soil microbes are able to produce VOCs from precursors in the soil and that the emissions observed were not just due to an abiotic release from soil. As shown in Figure 2, acetone was mainly consumed under wet soil conditions therefore, the emission observed for ^{13}C-enriched acetone during pre-drought demonstrated that soil microbes can both produce and consume acetone and that under wet conditions they were able to consume more acetone than they actually produced. During drought the emissions of ^{13}C-enriched acetone were about one order of magnitude higher than during pre-drought. This is a further evidence that under drought stress soil microbes used energy resources for a higher production of VOCs[26,55].

4. Discussion

In normal wet conditions, the soil of the experimental rainforest acted as a net VOC sink. The soil uptake capacity progressively decreased in response to increasing drought and, under severe drought conditions the soil started to be a strong source of several VOCs, including carbonyls and methyl nitrite. This trend could be attributable to the soil microbes that under drought stress significantly reduced their consumption of atmospheric VOCs, and to prevent osmotic imbalance, relocated carbon and nitrogen resources from growth pathways to produce and accumulate osmolytes, including VOCs[26,55]. This was further confirmed by the position specific ^{13}C-pyruvate experiments that clearly demonstrated that soil microbes can be a significant source of VOCs from available energy sources and that their energetic investment in VOCs production was higher during drought[55]. The moisture threshold below which the soil microbes dramatically reduced consumption of atmospheric VOCs and started to become a source of several VOCs was 19%. Currently the soil moisture conditions normally experienced in tropical rainforests such as the Amazon are higher. However, continued global warming, deforestation, and the predicted increased frequency of El Niño events is likely to reduce soil moisture levels to below this threshold for longer periods inducing strong associated emission events[16]. For instance, during the strong El Niño drought in 2015/2016 a negative soil moisture anomaly with an average reduction of almost 30% was reported in the Amazon basin and at same time large pulses of unexplained OH reactivity was observed in the same region[56,57]. Reduced soil VOC uptake capacity as well as increased soil and plant VOC emissions induced by the El Niño drought could represent a potential explanation for the OH reactivity pulse[57]. Therefore, the results shown in the present study have implications to near future real-world scenarios. Increased soil VOC emissions in combination with a reduction of the atmospheric VOCs uptake by the soil will strongly affect the

rainforest ecosystem atmospheric chemistry with possible further feedbacks on radiative effects and climate. These emission effects will be further exacerbated by soil rewetting events following prolonged drought periods as shown by the large pulse in soil VOC and CO_2 emissions observed after the rainfall events. The rewetting induced a fast mobilization of the soil organic carbon pools that resulted in a large and rapidly produced emission peak of carbonyl compounds. The subsequent microbial mineralization of these mobilized carbon sources resulted in a CO_2 pulse (Birch effect)[46]. The dimethyl sulfide emission pulse after soil rewetting was attributable to water-induced mobilization of the soil organic sulfur pools by soil microbes and enzymes. Dimethyl sulfide pulse occurred later than the carbonyls pulse, due to a slower mobilization of the sulfur pools than the carbon pools. The increase also observed in ambient concentrations simultaneously to the soil emission pulses, showed that soil can significantly contribute to dimethyl sulfide concentrations in the atmosphere. DMS is of high relevancy in atmospheric chemistry as it can be oxidized to condensable products that form secondary sulfate aerosols and contribute to new particle formation[34,58,59].

Soil fluxes of several VOCs followed a diel cycle with higher emission and uptake rates both occurring during daytime compared to nighttime. Soil uptake rates of isoprenoids closely followed the diel cycle of their atmospheric concentrations, while diel cycles in methyl nitrite emissions were a consequence of light dependent processes at or near to the soil surface. Considering the high relevance of methyl nitrite for the atmospheric chemistry due to its rapid photolysis to NO and formaldehyde[35] and considering that methyl nitrite emissions occurred only during drought, the presented results suggest that future climate change will also affect diel rainforest carbon cycles and the related atmospheric chemistry.

Prolonged drought and recovery had a major impact on soil VOC fluxes from the experimental rainforest, affecting the composition and quantity of VOCs in the atmosphere of the enclosed ecosystem[17]. Soil VOC fluxes and their parametrization related to soil moisture levels must be included in atmospheric models to simulate current atmospheric chemistry and to improve climate model predictions of ecosystem responses to drought.

5. Methods

5.1 The B2 TRF mesocosm and controlled drought experiment

The B2 TRF mesocosm is a fully enclosed ecosystem which allows temperature, humidity, atmospheric gas composition, and precipitation to be manipulated[18–20]. The mesocosm has an area of 1940 m^2 and a volume of 26700 m^3 and the vegetation is rooted in 2-4 m of soil (sandy clay loam: 20–35 % clay and >70 % sand). The low ozone (O_3) concentration (ca. 1 ppbV) and the reduced hydroxyl radicals (OH) formation inside the B2 TRF due the UV-light filtering by the glass, prevent VOCs oxidation. The enclosed air is therefore relatively rich in primary VOC emissions and relatively poor in oxidized

297 products. Isoprene and monoterpene concentrations measured in the ambient air of the B2 TRF were
298 respectively two orders and one order of magnitude higher than measurements in Earth's tropical rain
299 forest[60,61], which reflect the rate of reaction with OH and O_3. Therefore, the absence of atmospheric
300 chemistry makes the B2 TRF an ideal site to study VOC dynamics as it allows the estimation of soil
301 emission and uptake even of highly reactive VOCs.
302 The soil flux measurements were conducted during the Water, Atmosphere, and Life Dynamics
303 campaign (B2-WALD)[17] from September 2019 to January 2020 during which 65 days of drought were
304 induced. The campaign started with a pre-drought phase, with rainfall regime kept at a rate of about
305 30 mm per week. The drought phase started after the last rainfall event at midnight 7th October 2019.
306 From 1st November 2019 to 2nd December 2019 the relative humidity of the ecosystem was further
307 reduced enhancing the drought conditions. After 65 days of drought, at 5:30 am on 12 December
308 2019, 3 soil chambers placed on 3 different sites of the B2 TRF were manually rewet by adding ~2.2 L
309 (~22.5 mm) of water per chamber. Soil fluxes from these chambers were measured with a high
310 frequency, i.e. each chamber was measured every 30 minutes for 5 hours, with the aim to capture fast
311 soil flux rewet dynamics. Rainout shelters were placed over the 3 manually rewetted chambers while,
312 at 11 am on 12 December 2019, the remaining 9 chambers were subjected to the whole forest rewet.
313 From 30 minutes before the whole forest rewet, all the 12 chambers were measured consecutively
314 with a temporal resolution of 2 hours. Precipitation was delivered via overhead sprinklers and ~35000
315 L (~18 mm) of water were added over 4.5 hours period. A second rainfall event on the whole forest
316 involving all 12 soil chambers was conducted one week later on 19 December 2019 at 11:00, by adding
317 ~ 36000 L (~19 mm) of water in 4.5 hours. Subsequent rain events were then conducted every second
318 day starting from midnight on 21 December.

319 ## 5.2 Experimental set-up

320 Soil VOC fluxes were measured continuously using a proton transfer time of flight mass spectrometer
321 (PTR-ToF-MS-8000, Ionicon Analytik GmbH, Innsbruck, Austria) directly connected to the outflow of
322 an automated soil flux measuring system consisting of a LI-8100 infrared gas analyzer (IRGA; for CO_2
323 fluxes measurement), a LI-8150 16-port multiplexer (Licor Inc., Lincoln, NA, USA) and 12 dynamic soil
324 flux chambers (LI 8100-104 Long-Term Chambers with opaque lids, Licor Inc.). A detailed description
325 and the working principle of the PTR-ToF-MS instrument can be found elsewhere[62]. Concisely, the soft
326 ionization process is based on a proton transfer from hydronium ions (H_3O^+) to sample VOCs having a
327 higher proton affinity than water (691 kJ mol^{-1}). Protonated VOCs are then analyzed in a high-
328 resolution time-of-flight mass spectrometer according to mass-to-charge ratio (*m/z*). The instrumental
329 settings were as follows. The PTR drift tube pressure was 2.2 mbar, the PTR drift tube voltage was 600

V, and the PTR drift tube temperature was 60 °C, resulting in an E/N ratio of 137 Td. The time resolution was 10 s with the *m/z* monitored up to 500 Da.

The total volume of the soil flux system, including chamber, tubing, IRGA and multiplexer, was about 6.5-7 L. For gas analysis, ca. 100 sccm were subsampled from the LI-8100A outflow and distributed to the different analyzers including the PTR for VOCs measurement. To avoid a negative pressure, ca. 100 sccm of synthetic air were introduced in the soil flux system. In order to minimize surface effects on VOC analysis, perfluoroalkoxy (PFA) tubing was used for the soil flux system, for the subsampling line and for the PTR inlet[63]. The PTR sampling flow was 30 sccm and the PTR inlet temperature was 60 °C. All PTR-TOF files were processed using the software PTRwid[64]. The ion yields of all *m/z* were measured in counts per second (cps) and compounds were identified from the measured exact *m/z* of their protonated parent ions and isotopic patterns. To account for possible variations of the reagent ion signals, measured ion intensities were normalized to the H_3O^+ counts in combination with the water-cluster ion counts[65]. Only compounds with signal intensities higher than the instrumental background were considered for further analysis.

Nocturnal calibrations, starting from midnight, were performed using a standard gas cylinder containing different multi-VOC component calibration mixtures in Ultra-High Purity (UHP) nitrogen (Apel-Riemer Environmental, Inc., Colorado, USA). The VOC mix was subjected to 5-step dynamic dilutions by means of a liquid calibration unit (LCU, IONICON Analytik, Innsbruck, Austria). The gas standard was equilibrated in the LCU for one hour prior to the start of calibration. The zero-air flow was held constant at 1000 sccm, while the gas standard flow was changed every 15 min starting from 40 sccm until 0 sccm in 10 sccm steps. To calibrate at same humidity level observed in the B2 TRF, 20 µL/min of milli-Q water were dynamically nebulized into the evaporation chamber of the LCU.

The two calibration standard cylinders were used during the campaign to allow explicit calibration of a wide range of species. The first cylinder was used for two periods: from 18 September 2019 to 6 November 2019; and from 17 December 2019 to 20 January 2020. The second cylinder was used from 7 November 2019 to 16 December 2019. VOC gas standards for daily calibration included in the two calibration standard cylinders with their respective detection limit (LOD) and total uncertainty are reported in table S1. Concentrations of compounds not included in the calibration standard cylinders were calculated applying the kinetic theory of proton transfer reaction with an uncertainty of ≤50%[65]. Ions that showed measurable soil fluxes are reported in table S2, along with tentative identifications for the underlying VOC species based on previous literature[66]. For methyl nitrite (CH_3ONO), the contribution of ion signal from the ^{13}C isotopologue of acetic acid ($C_2H_4O_2^+$) at *m/z* 61.0284 was subtracted from the ion signal at *m/z* 62.029. The interference of the ^{13}C isotopologue also explains the lower mass accuracy for methyl nitrite detection.

In addition, chemical speciation of monoterpene soil fluxes was performed by means of gas chromatography time of flight mass spectrometry (GC-ToF-MS) and three manual soil chambers. Details of the method used for monoterpenes speciation are reported in the supplementary information.

5.3 Soil fluxes measurements

The 12 chambers were placed on PVC-collars (Ø: 20 cm) installed at 2-3 cm depth at four different sites of the B2 TRF on vegetation-free, bare soil eight weeks before the start of the measurements. Each chamber measurement consisted of 2.5 minutes of pre-purge during which the chamber lid was open and lines flushed with the ambient air, 6.5 minutes of closure time and 1 minute of post-purge for a total measurement time of 10 minutes. All 12 chambers were measured consecutively resulting in a temporal resolution of 2 hours. Soil VOC fluxes were calculated by applying the linear regression model to the VOC concentrations measured during the 6.5 minute of chamber closure. The first 30 s after chamber closure were discarded due to possible perturbations induced by the closure and the linear regression was applied to the successive 100 s. The slope of the linear regression was divided by chamber area, and a time factor to convert the results to hourly units.

Soil CO_2 fluxes were calculated with linear and exponential models, fitted to each individual chamber measurement. In the same way as the VOC fluxes, the first 30 s after chamber closure were omitted and the linear model was applied to the successive 120 s, while the exponential model was applied to the full closure time. The linear model was only used in case the algorithm failed to fit the exponential model.

5.4 ^{13}C pyruvate labeling

To identify origin of emitted VOCs, soil was labeled with position specific $^{13}C_1$-pyruvate and $^{13}C_2$-pyruvate. Position specific ^{13}C-labelled pyruvate is a powerful tracker because it serves as substrate for primary and secondary metabolic pathways as the C_1-carbon position of pyruvate is decarboxylated while the remaining acetyl-CoA can be involved in VOC biosynthesis [67–69]. ^{13}C-pyruvate was added in 9 soil chambers located within three sites in B2 TRF during pre-drought from 12th to 15th September and during severe drought from 7th to 19th November. Each morning, the chambers were labeled at around 10 AM with $^{13}C_1$-pyruvate or $^{13}C_2$-pyruvate. A 5x5 cm metal frame with 1x1cm openings was placed into the PVC-collar of each chamber into which 100 µl at concentration 40 mg/ml of C_1-^{13}C-pyruvate or C_2-^{13}C-pyruvate solution was added to each 1x1 cm opening to a depth of 1 cm, for a total of 25 injections per chamber[55]. After pyruvate injections, chambers were measured every 30 minutes for the first 8 hours and then were measured every 50 minutes until 48 h post labeling. The isotopic composition of the flux rate was calculated by applying the linear model to the fractional abundance of ^{13}C defined as: ^{13}C-VOC/(^{13}C-VOC +^{12}C-VOC).

5.5 Soil sensors

Soil moisture and temperature sensors (SMT100, Truebner Gmbh, Neustadt, Germany) and soil matric potential sensors (TEROS 21, Meter Group, Pullman, WA, USA) were installed in 5 cm soil depth from the soil surface close to the soil chamber sites.

5.6 Statistical analysis

Thresholds in the relationship of soil moisture and VOC fluxes and deposition velocities were identified performing segmented regression analysis on daily averaged values[70]. Threshold models were only considered if the AIC of the model was lower than of the corresponding linear model. Threshold model estimation was repeated with 1000 bootstrapped samples to estimate the distribution of the thresholds. The analysis was performed using R (version 4.1.1.) and the package chngpt[70].

6. References

1. Scott, C. E. *et al.* Impact on short-lived climate forcers increases projected warming due to deforestation. *Nat Commun* **9**, 157 (2018).
2. Guenther, A. B. *et al.* The Model of Emissions of Gases and Aerosols from Nature version 2.1 (MEGAN2.1): an extended and updated framework for modeling biogenic emissions. *Geoscientific Model Development* **5**, 1471–1492 (2012).
3. Acosta Navarro, J. C. *et al.* Global emissions of terpenoid VOCs from terrestrial vegetation in the last millennium. *J Geophys Res Atmos* **119**, 6867–6885 (2014).
4. Hakola, H. *et al.* Seasonal variation of VOC concentrations above a boreal coniferous forest. *Atmospheric Environment* **37**, 1623–1634 (2003).
5. Kramshøj, M. *et al.* Large increases in Arctic biogenic volatile emissions are a direct effect of warming. *Nature Geosci* **9**, 349–352 (2016).
6. Bourtsoukidis, E. *et al.* Strong sesquiterpene emissions from Amazonian soils. *Nat Commun* **9**, 2226 (2018).
7. Staudt, M., Byron, J., Piquemal, K. & Williams, J. Compartment specific chiral pinene emissions identified in a Maritime pine forest. *Science of The Total Environment* **654**, 1158–1166 (2019).

8. Moldrup, P., Olesen, T., Schjønning, P., Yamaguchi, T. & Rolston, D. E. Predicting the Gas Diffusion Coefficient in Undisturbed Soil from Soil Water Characteristics. *Soil Science Society of America Journal* **64**, 94–100 (2000).
9. Gray, C. M., Monson, R. K. & Fierer, N. Biotic and abiotic controls on biogenic volatile organic compound fluxes from a subalpine forest floor. *Journal of Geophysical Research: Biogeosciences* **119**, 547–556 (2014).
10. Gray, C. M., Helmig, D. & Fierer, N. Bacteria and fungi associated with isoprene consumption in soil. *Elementa: Science of the Anthropocene* **3**, 000053 (2015).
11. Asensio, D., Peñuelas, J., Filella, I. & Llusià, J. On-line screening of soil VOCs exchange responses to moisture, temperature and root presence. *Plant Soil* **291**, 249–261 (2007).
12. Aaltonen, H. *et al.* Continuous VOC flux measurements on boreal forest floor. *Plant Soil* **369**, 241–256 (2013).
13. Rossabi, S., Choudoir, M., Helmig, D., Hueber, J. & Fierer, N. Volatile Organic Compound Emissions From Soil Following Wetting Events. *J. Geophys. Res. Biogeosci.* **123**, 1988–2001 (2018).
14. Mu, Z. *et al.* Seasonal and diurnal variations of plant isoprenoid emissions from two dominant species in Mediterranean shrubland and forest submitted to experimental drought. *Atmospheric Environment* **191**, 105–115 (2018).
15. Mäki, M., Krasnov, D., Hellén, H., Noe, S. M. & Bäck, J. Stand type affects fluxes of volatile organic compounds from the forest floor in hemiboreal and boreal climates. *Plant Soil* **441**, 363–381 (2019).
16. Lee, J.-Y. *et al.* Future global climate: scenario-based projections and near-term information. in *Climate Change 2021: The Physical Science Basis. Contribution of Working Group I to the Sixth Assessment Report of the Intergovernmental Panel on Climate Change* (eds. Masson-Delmotte, V. et al.) (Cambridge University Press, 2021).

17. Werner, C. *et al.* Ecosystem fluxes during drought and recovery in an experimental forest. *Science* **374**, 1514–1518 (2021).
18. Pegoraro, E. *et al.* The effect of elevated atmospheric CO2 and drought on sources and sinks of isoprene in a temperate and tropical rainforest mesocosm. *Global Change Biology* **11**, 1234–1246 (2005).
19. Pegoraro, E., Rey, A., Abrell, L., Van Haren, J. & Lin, G. Drought effect on isoprene production and consumption in Biosphere 2 tropical rainforest. *Global Change Biology* **12**, 456–469 (2006).
20. Van Haren, J. L. M. *et al.* Drought-induced nitrous oxide flux dynamics in an enclosed tropical forest. *Global Change Biology* **11**, 1247–1257 (2005).
21. Siebielec, S. *et al.* Impact of Water Stress on Microbial Community and Activity in Sandy and Loamy Soils. *Agronomy* **10**, 1429 (2020).
22. Cleveland, C. & Yavitt, J. Consumption of atmospheric isoprene in soil. *Geophysical Research Letters - GEOPHYS RES LETT* **24**, 2379–2382 (1997).
23. Byron, J. *et al. Chiral monoterpenes reveal forest emission mechanisms and drought responses*. https://www.researchsquare.com/article/rs-770148/v1 (2021) doi:10.21203/rs.3.rs-770148/v1.
24. Hayward, S., Muncey, R. J., James, A. E., Halsall, C. J. & Hewitt, C. N. Monoterpene emissions from soil in a Sitka spruce forest. *Atmospheric Environment* **35**, 4081–4087 (2001).
25. Asensio, D. *et al.* Interannual and seasonal changes in the soil exchange rates of monoterpenes and other VOCs in a Mediterranean shrubland. *European Journal of Soil Science* **59**, 878–891 (2008).
26. Schimel, J., Balser, T. C. & Wallenstein, M. Microbial Stress-Response Physiology and Its Implications for Ecosystem Function. *Ecology* **88**, 1386–1394 (2007).
27. Kolb, S. Aerobic methanol-oxidizing *Bacteria* in soil. *FEMS Microbiology Letters* **300**, 1–10 (2009).
28. Stacheter, A. *et al.* Methanol oxidation by temperate soils and environmental determinants of associated methylotrophs. *ISME J* **7**, 1051–1064 (2013).

29. Kramshøj, M. *et al.* Biogenic volatile release from permafrost thaw is determined by the soil microbial sink. *Nat Commun* **9**, 3412 (2018).
30. Trowbridge, A. M., Stoy, P. C. & Phillips, R. P. Soil Biogenic Volatile Organic Compound Flux in a Mixed Hardwood Forest: Net Uptake at Warmer Temperatures and the Importance of Mycorrhizal Associations. *Journal of Geophysical Research: Biogeosciences* **125**, e2019JG005479 (2020).
31. Kesselmeier, J. & Hubert, A. Exchange of reduced volatile sulfur compounds between leaf litter and the atmosphere. *Atmospheric Environment* **36**, 4679–4686 (2002).
32. Schäfer, H., Myronova, N. & Boden, R. Microbial degradation of dimethylsulphide and related C1-sulphur compounds: organisms and pathways controlling fluxes of sulphur in the biosphere. *Journal of Experimental Botany* **61**, 315–334 (2010).
33. Mancuso, S. *et al.* Soil volatile analysis by proton transfer reaction-time of flight mass spectrometry (PTR-TOF-MS). *Applied Soil Ecology* **86**, 182–191 (2015).
34. Jardine, K. *et al.* Dimethyl sulfide in the Amazon rain forest. *Global Biogeochemical Cycles* **29**, 19–32 (2015).
35. Taylor, W. D. *et al.* Atmospheric photodissociation lifetimes for nitromethane, methyl nitrite, and methyl nitrate. *International Journal of Chemical Kinetics* **12**, 231–240 (1980).
36. Stevenson, F. J. & Swaby, R. J. Nitrosation of Soil Organic Matter: I. Nature of Gases Evolved During Nitrous Acid Treatment of Lignins and Humic Substances. *Soil Science Society of America Journal* **28**, 773–778 (1964).
37. Magalhães, A. M. T. & Chalk, P. M. Factors affecting formation of methyl nitrite in soils. *Journal of Soil Science* **38**, 701–709 (1987).
38. Su, H. *et al.* Soil nitrite as a source of atmospheric HONO and OH radicals. *Science* **333**, 1616–1618 (2011).
39. Oswald, R. *et al.* HONO Emissions from Soil Bacteria as a Major Source of Atmospheric Reactive Nitrogen. *Science* **341**, 1233–1235 (2013).

40. Weber, B. *et al.* Biological soil crusts accelerate the nitrogen cycle through large NO and HONO emissions in drylands. *Proceedings of the National Academy of Sciences* **112**, 15384–15389 (2015).
41. Ermel, M. *et al.* Hydroxylamine released by nitrifying microorganisms is a precursor for HONO emission from drying soils. *Sci Rep* **8**, 1877 (2018).
42. Manzoni, S., Schimel, J. P. & Porporato, A. Responses of soil microbial communities to water stress: results from a meta-analysis. *Ecology* **93**, 930–938 (2012).
43. Birch, H. F. The effect of soil drying on humus decomposition and nitrogen availability. *Plant Soil* **10**, 9–31 (1958).
44. Jarvis, P. *et al.* Drying and wetting of Mediterranean soils stimulates decomposition and carbon dioxide emission: the 'Birch effect'. *Tree Physiology* **27**, 929–940 (2007).
45. Borken, W. & Matzner, E. Reappraisal of drying and wetting effects on C and N mineralization and fluxes in soils. *Global Change Biology* **15**, 808–824 (2009).
46. Unger, S., Máguas, C., Pereira, J. S., David, T. S. & Werner, C. The influence of precipitation pulses on soil respiration – Assessing the "Birch effect" by stable carbon isotopes. *Soil Biology and Biochemistry* **42**, 1800–1810 (2010).
47. Navarro-García, F., Casermeiro, M. Á. & Schimel, J. P. When structure means conservation: Effect of aggregate structure in controlling microbial responses to rewetting events. *Soil Biology and Biochemistry* **44**, 1–8 (2012).
48. Strickland, T. C. & Fitzgerald, J. W. Formation and mineralization of organic sulfur in forest soils. *Biogeochemistry* **1**, 79–95 (1984).
49. Watwood, M. E., Fitzgerald, J. W. & Gosz, J. R. Sulfur processing in forest soil and litter along an elevational and vegetative gradient. *Can. J. For. Res.* **16**, 689–695 (1986).
50. Lado-Monserrat, L., Lull, C., Bautista, I., Lidón, A. & Herrera, R. Soil moisture increment as a controlling variable of the "Birch effect". Interactions with the pre-wetting soil moisture and litter addition. *Plant Soil* **379**, 21–34 (2014).

51. Canarini, A., Kiær, L. P. & Dijkstra, F. A. Soil carbon loss regulated by drought intensity and available substrate: A meta-analysis. *Soil Biology and Biochemistry* **112**, 90–99 (2017).
52. Rubio, V. E. & Detto, M. Spatiotemporal variability of soil respiration in a seasonal tropical forest. *Ecology and Evolution* **7**, 7104–7116 (2017).
53. Meusel, H. *et al.* Emission of nitrous acid from soil and biological soil crusts represents an important source of HONO in the remote atmosphere in Cyprus. *Atmospheric Chemistry and Physics* **18**, 799–813 (2018).
54. Tsai, C. *et al.* Nitrous acid formation in a snow-free wintertime polluted rural area. *Atmos. Chem. Phys.* **18**, 1977–1996 (2018).
55. Honeker, L. *et al. Drought induces soil microbial stress responses and emissions of volatile organic compounds in an artificial tropical rainforest*. https://www.researchsquare.com/article/rs-1840246/v1 (2022) doi:10.21203/rs.3.rs-1840246/v1.
56. van Schaik, E. *et al.* Changes in surface hydrology, soil moisture and gross primary production in the Amazon during the 2015/2016 El Niño. *Philosophical Transactions of the Royal Society B: Biological Sciences* **373**, 20180084 (2018).
57. Pfannerstill, E. Y. *et al.* Total OH Reactivity Changes Over the Amazon Rainforest During an El Niño Event. *Frontiers in Forests and Global Change* **1**, (2018).
58. Veres, P. R. *et al.* Global airborne sampling reveals a previously unobserved dimethyl sulfide oxidation mechanism in the marine atmosphere. *Proceedings of the National Academy of Sciences* **117**, 4505–4510 (2020).
59. Fung, K. M. *et al.* Exploring dimethyl sulfide (DMS) oxidation and implications for global aerosol radiative forcing. *Atmospheric Chemistry and Physics* **22**, 1549–1573 (2022).
60. Karl, T. *et al.* Exchange processes of volatile organic compounds above a tropical rain forest: Implications for modeling tropospheric chemistry above dense vegetation. *Journal of Geophysical Research: Atmospheres* **109**, (2004).

61. Yáñez-Serrano, A. M. *et al.* Diel and seasonal changes of biogenic volatile organic compounds within and above an Amazonian rainforest. *Atmos. Chem. Phys.* **15**, 3359–3378 (2015).
62. Jordan, A. *et al.* A high resolution and high sensitivity proton-transfer-reaction time-of-flight mass spectrometer (PTR-TOF-MS). *International Journal of Mass Spectrometry* **286**, 122–128 (2009).
63. Deming, B. L. *et al.* Measurements of delays of gas-phase compounds in a wide variety of tubing materials due to gas–wall interactions. *Atmospheric Measurement Techniques* **12**, 3453–3461 (2019).
64. Holzinger, R. PTRwid: A new widget tool for processing PTR-TOF-MS data. *Atmospheric Measurement Techniques* **8**, 3903–3922 (2015).
65. de Gouw, J. *et al.* Sensitivity and specificity of atmospheric trace gas detection by proton-transfer-reaction mass spectrometry. *International Journal of Mass Spectrometry* **223–224**, 365–382 (2003).
66. Yáñez-Serrano, A. M. *et al.* Amazonian biogenic volatile organic compounds under global change. *Global Change Biology* **26**, 4722–4751 (2020).
67. Priault, P., Wegener, F. & Werner, C. Pronounced differences in diurnal variation of carbon isotope composition of leaf respired CO2 among functional groups. *New Phytologist* **181**, 400–412 (2009).
68. Kreuzwieser, J. *et al.* Drought affects carbon partitioning into volatile organic compound biosynthesis in Scots pine needles. *New Phytol* **232**, 1930–1943 (2021).
69. Werner, C., Fasbender, L., Romek, K. M., Yáñez-Serrano, A. M. & Kreuzwieser, J. Heat Waves Change Plant Carbon Allocation Among Primary and Secondary Metabolism Altering CO2 Assimilation, Respiration, and VOC Emissions. *Frontiers in Plant Science* **11**, (2020).
70. Fong, Y., Huang, Y., Gilbert, P. B. & Permar, S. R. chngpt: threshold regression model estimation and inference. *BMC Bioinformatics* **18**, 454 (2017).

7. Acknowledgements

This research was funded by the European Research Council (ERC; Grant Number 647008 (VOCO2)) to C.W and from the Philecology Foundation to Biosphere 2 to L.M. G. P. was supported by the German Federal Ministry of Education and Research (BMBF contract 01LB1001A – ATTO+) and the Max Planck Society.

8. Author contributions

GP analyzed the data, prepared and interpreted the results, and wrote the paper. JI, LM, TK, JvH, JK, CW, JW designed the experimental set-up. JI, LM, EYP, KM, JB, JGL, NL, CW performed the experiments. NL, LM, CW and JW supervised and conceived the experiments. All authors contributed to writing and editing the manuscript.

9. Competing interest

The authors declare no competing interests

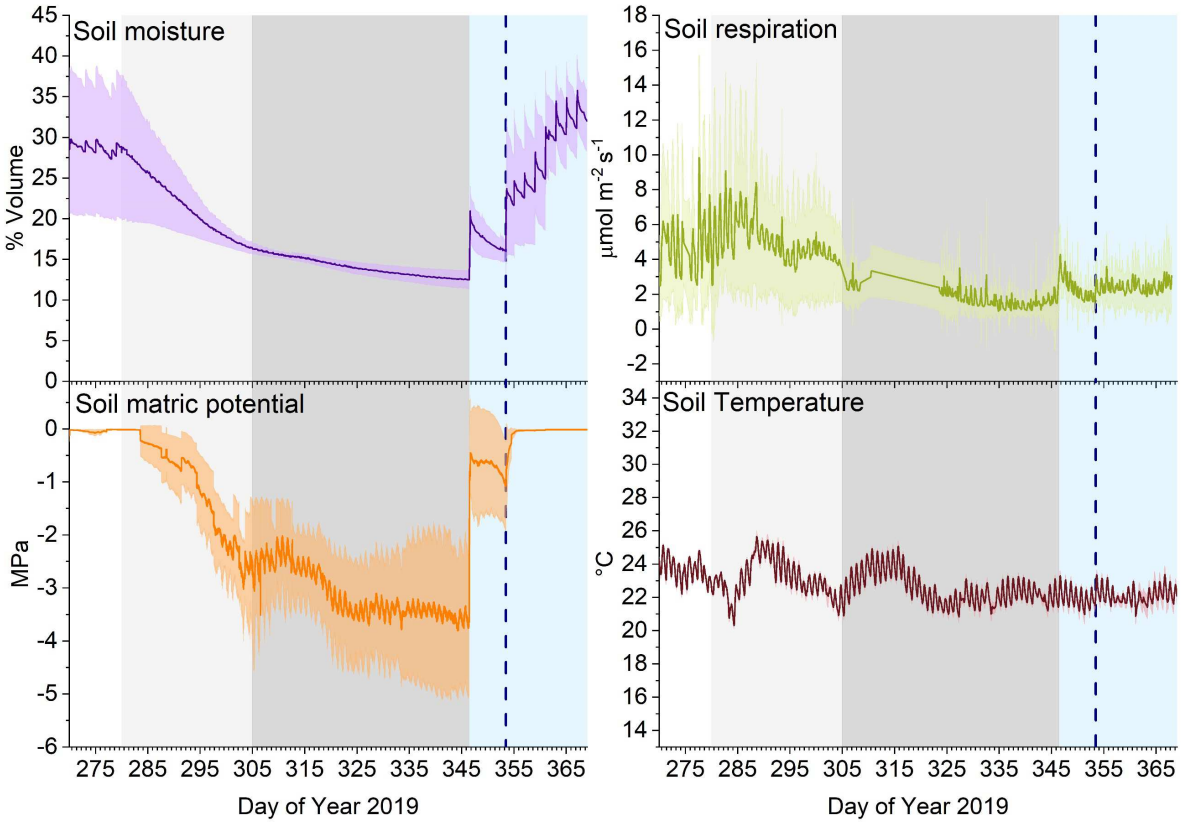

Figure 1 *Time series of soil moisture, soil matric potential, soil respiration and soil temperature. For soil respiration, line represents averaged value over all 12 soil chambers. For soil temperature, moisture and matric potential, lines represent averaged values over four sensors at 5 cm soil depth. The shaded areas indicate the standard deviation. Background colors indicate the different phases of the campaign: pre-drought (white), early drought (light gray), severe drought (dark gray), and recovery (light blue). The first drought-ending rain event occurred at the start of the recovery period, and the vertical blue line indicates the time of the second rain event.*

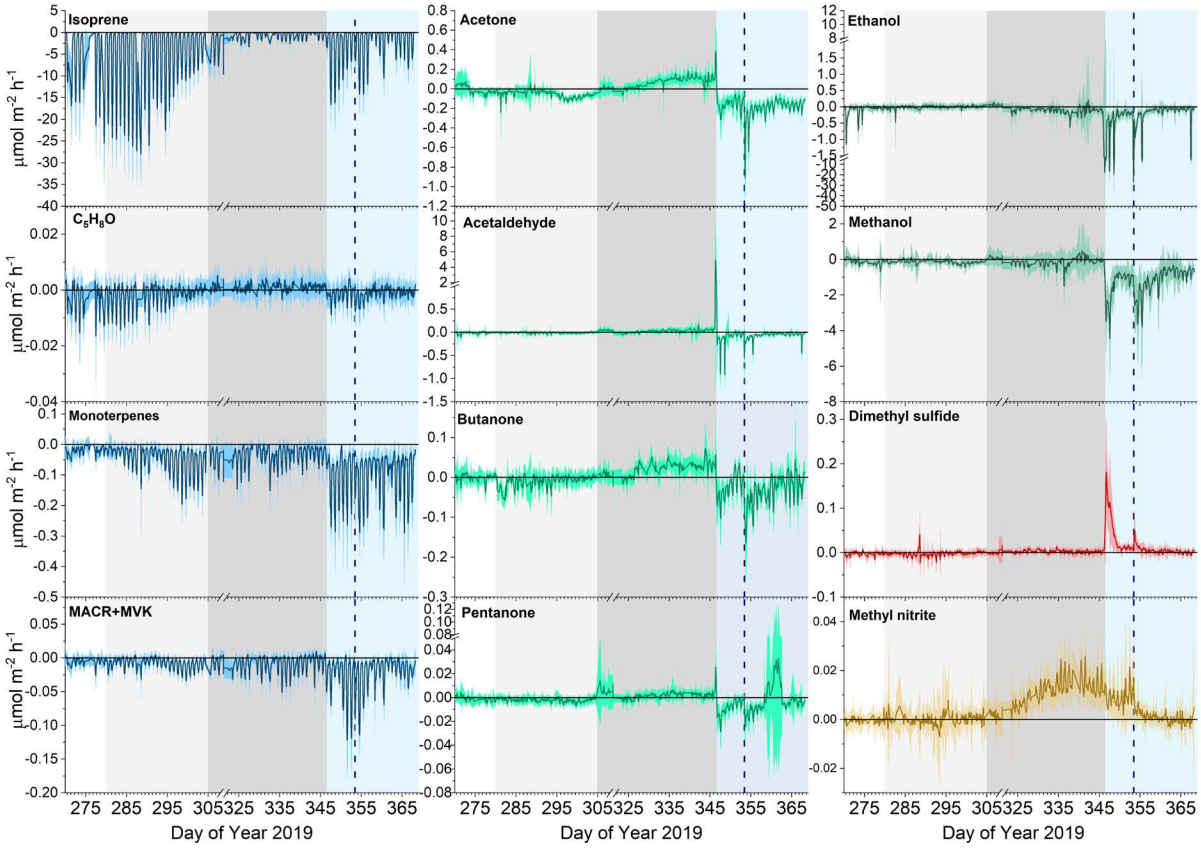

Figure 2 *Time series of soil VOC fluxes. Lines represent averaged fluxes over the all 12 chambers. The shaded areas indicate the standard deviation. Background colors indicate the different phases of the campaign: pre-drought (white), early drought (light gray), severe drought (dark gray), and recovery (light blue). The first drought-ending rain event occurred at the start of the recovery period, and the vertical blue line indicates the time of the second rain event.*

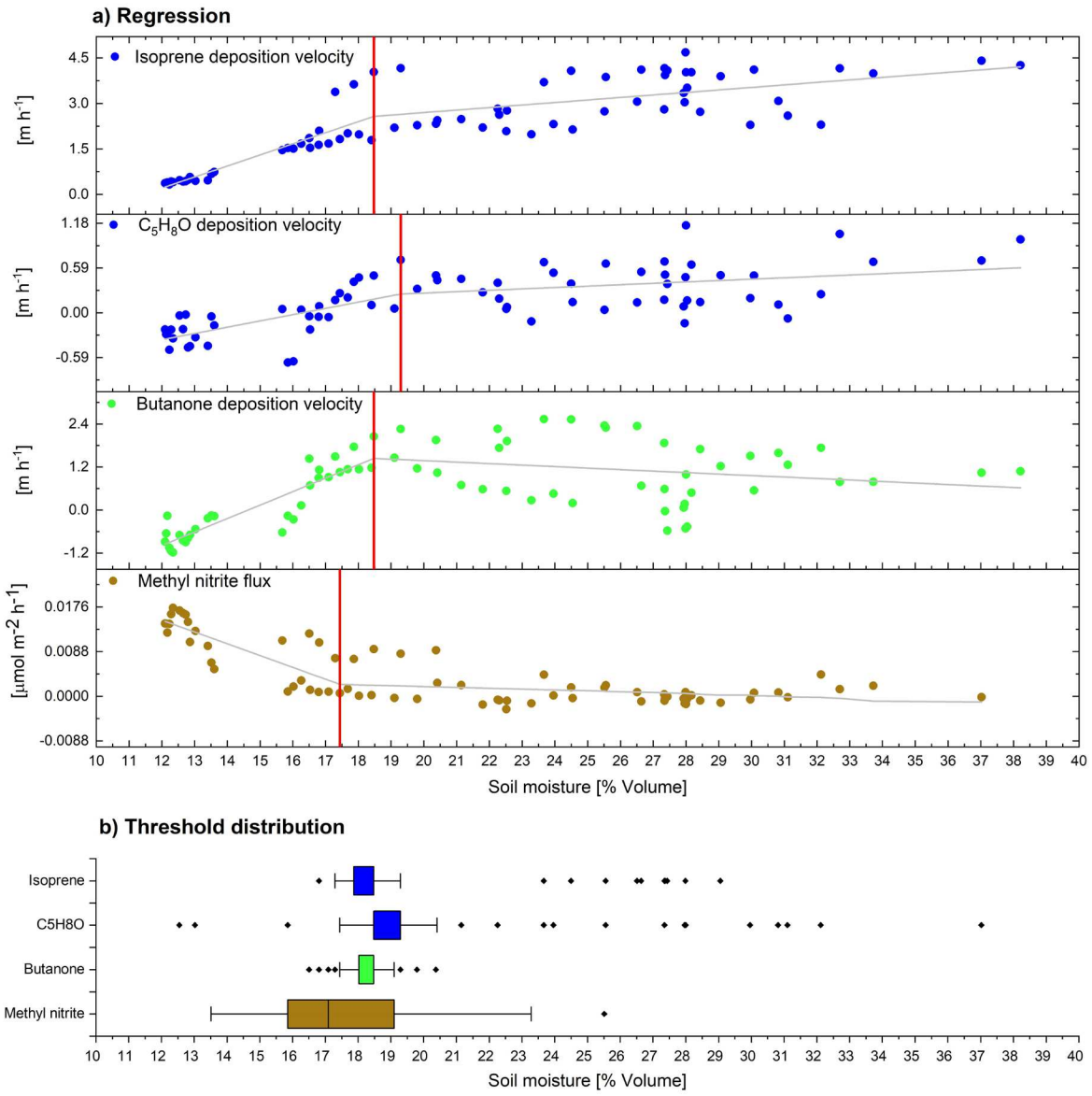

Figure 3 *Relationships of isoprene, C_5H_8O, butanone soil deposition velocity and methyl nitrite soil fluxes with soil moisture during the whole period of the campaign. Daily averaged values were used for all variables. Grey lines indicate the segmented regression model with the threshold indicated by the vertical red line (panel a). Distribution of threshold estimates based on 1000 bootstrapped samples (panel b).*

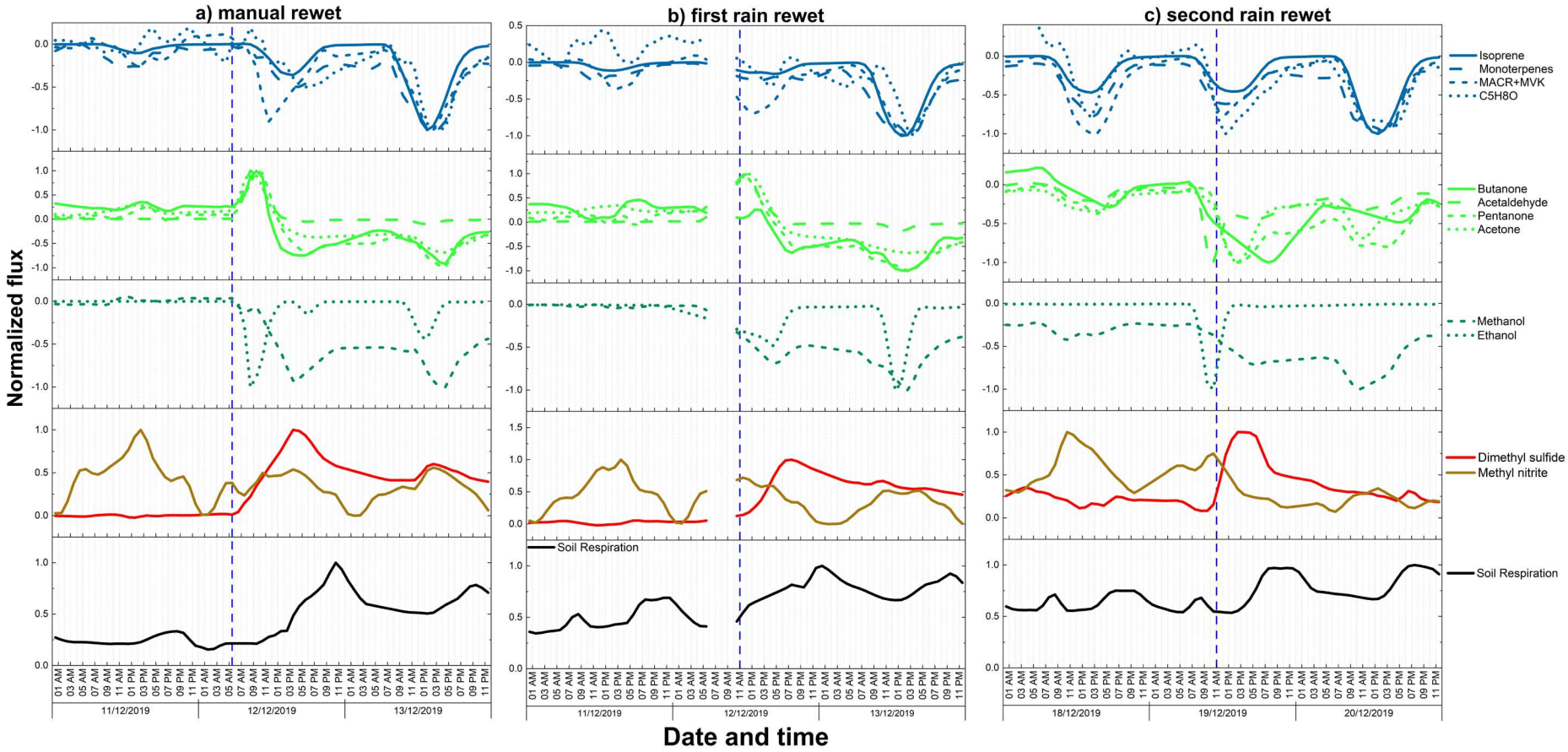

Figure 4 *Rewet dynamics for soil respiration and VOC soil fluxes after the manual rewet (a), the first rain rewet (b) and the second rain rewet (c). To make comparable the dynamics of different compounds, for each compound, soil fluxes were normalized to their respective absolute maximum. The data gap on the first rain rewet plots is due to the fact that during that time only the manual rewetted chambers were measured with a high temporal resolution with the aim to capture the fast dynamics.*

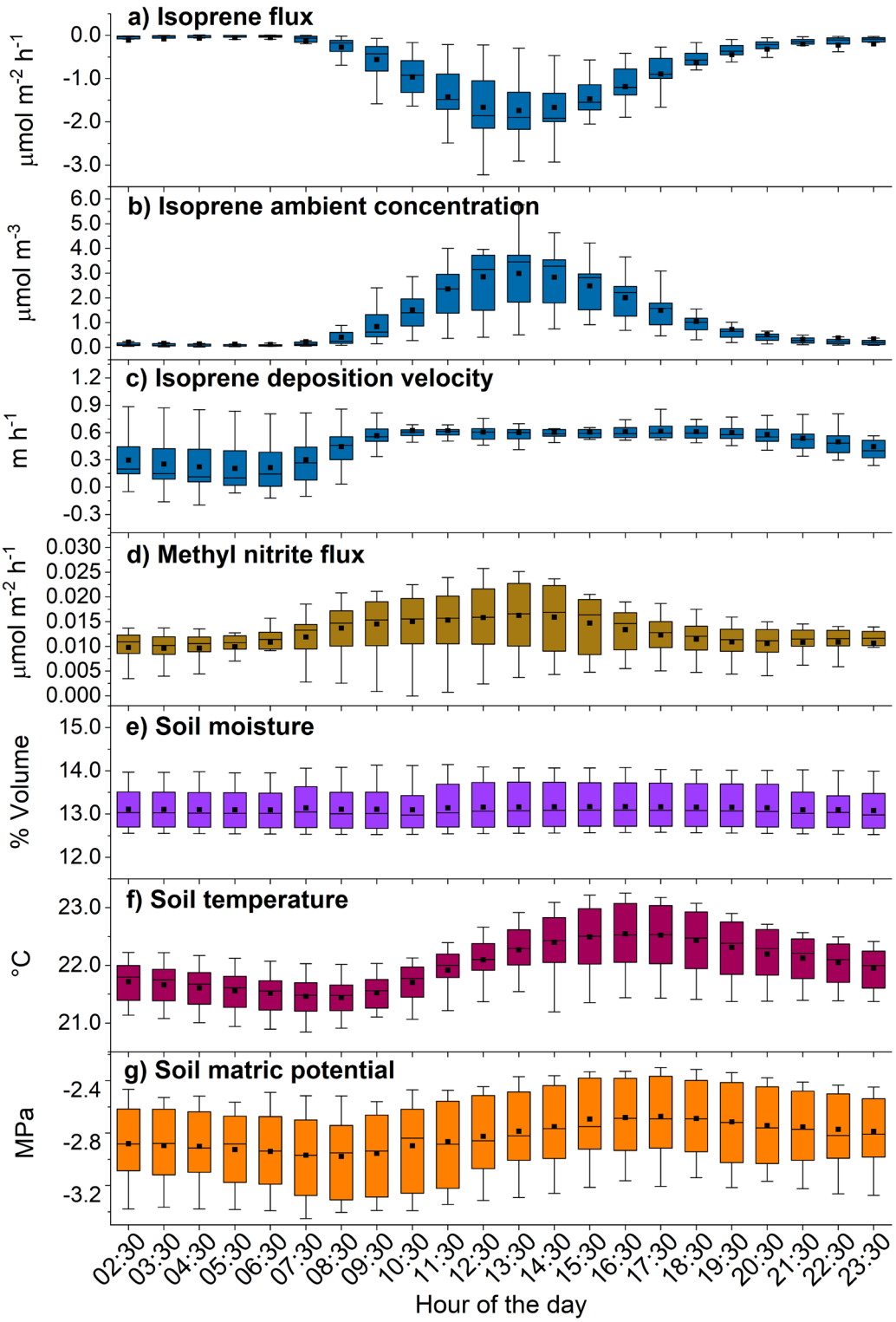

Figure 5 *Diel cycle observed during severe drought period (from doy 305 to doy 345) for a) isoprene soil flux, b) isoprene ambient concentration, c) isoprene deposition velocity, d) methyl nitrite flux, e) soil moisture, f) temperature, and g) soil matric potential. The boxes represent 25% to 75% of the dataset. The square dots and central lines indicate the mean and median values, respectively. The whiskers indicate the minimum and maximum data points.*

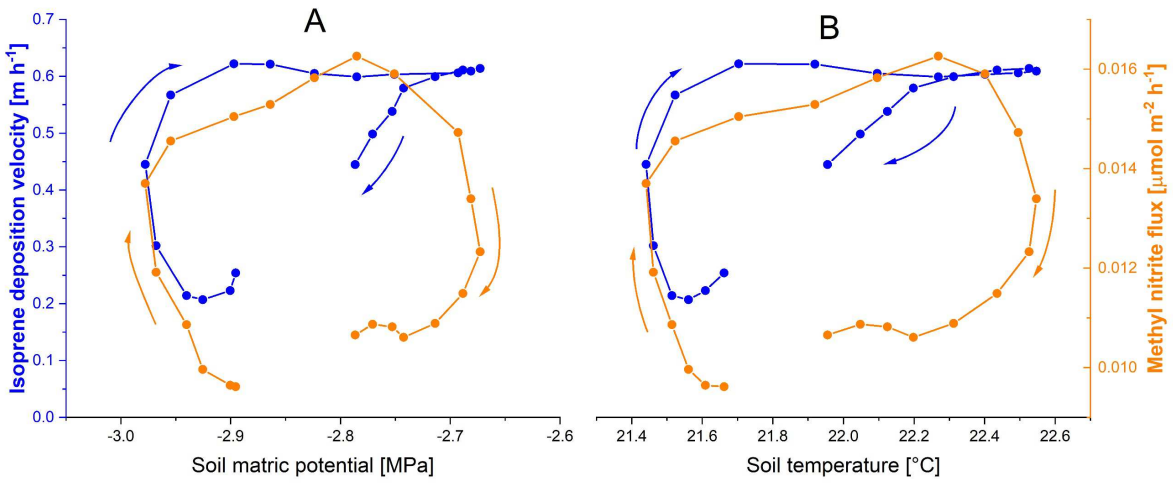

Figure 6 *Relationships of hourly averaged values of isoprene soil deposition (blue) and methyl nitrite emission (orange) with soil matric potential (panel A) and soil temperature (panel B).*

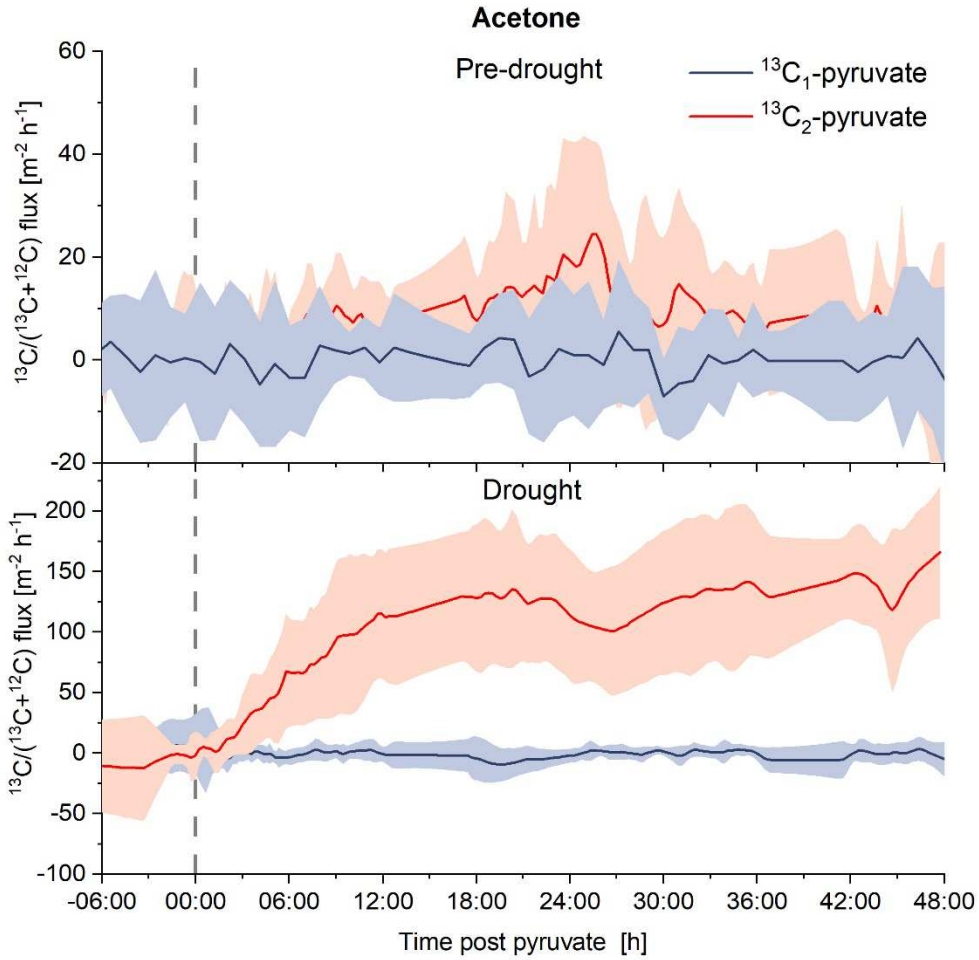

Figure 7 *^{13}C enrichment in acetone soil fluxes after the C_1-^{13}C-pyruvate (blue lines) and C_2-^{13}C-pyruvate (red lines) soil injections during drought (upper panel) and pre-drought (lower panel) period. Lines represent averaged fluxes over the 9 chambers. The shaded areas indicate the standard deviation.*

Supplementary Files

This is a list of supplementary files associated with this preprint. Click to download.

- Supplementaryinformation.docx